



CHORUS

This is the accepted manuscript made available via CHORUS. The article has been published as:

Femtosecond laser amorphization of tellurium

Yu-Hsiang Cheng, Samuel W. Teitelbaum, Frank Y. Gao, and Keith A. Nelson

Phys. Rev. B **98**, 134112 — Published 24 October 2018

DOI: [10.1103/PhysRevB.98.134112](https://doi.org/10.1103/PhysRevB.98.134112)

Femtosecond laser amorphization of tellurium

Yu-Hsiang Cheng, Samuel W. Teitelbaum, Frank Y. Gao, and Keith A. Nelson

Massachusetts Institute of Technology

(Dated: October 11, 2018)

Polycrystalline tellurium becomes amorphous after irradiation with strong femtosecond pulses. The amorphization is sensitive to the initial temperature but not very sensitive to the temporal profile of the optical excitation. Above the amorphization threshold, single-shot transient reflectivity traces show clear coherent phonon oscillations within 1 ps. These results suggest that amorphization is due to thermal melting rather than nonthermal melting or switching for pump fluences up to the ablation threshold.

I. INTRODUCTION

Laser-solid interactions in the femtosecond time regime have been studied extensively for both applications and fundamental insights. Femtosecond laser pulses can quickly produce a high density of carriers in semiconductors, and the hot carriers modify the interatomic potential such that atoms can move large distances even while the lattice remains cold. With excited carrier densities up to $\sim 10\%$ of the valence electrons, structural phase transitions can occur on a timescale of 100 fs^{1,2}, an order of magnitude faster than the picosecond timescales typical of energy relaxation from carriers to the lattice. Ultrafast nonthermal melting has been demonstrated in several semiconductors and semimetals such as Si³, GaAs⁴, Ge⁵, InSb⁶, and Bi⁷, and the reported melting time was fluence-dependent. In Si and GaAs⁴, such ultrafast behavior clearly occurs with fluence twice that of the melting threshold. More recently, researchers found that Ge₂Sb₂Te₅ (GST), a phase-change material, could undergo an ultrafast crystalline-to-amorphous phase transition upon femtosecond pulse irradiation without melting^{8,9}.

Tellurium is a semiconductor that can be switched reversibly between crystalline and amorphous phases by optical illumination¹⁰⁻¹⁴. The amorphous phase has lower reflectivity and lower optical absorption at 1.55 eV ($\lambda = 800$ nm) than the crystalline phase^{15,16}. The instability of the amorphous phase above 283 K¹⁶ limits its practical applications for data storage, but the single-element nature and relatively simple crystal structure of Te (only three atoms per unit cell) compared to phase-change memory alloys makes it an attractive target for fundamental studies of laser-induced phase transitions. Pamler and Marinero showed that the phase transition induced by nanosecond pulses is purely thermal¹⁴. With femtosecond excitation, Ashitkov et al. demonstrated loss in optical anisotropy after ~ 1 ps and attributed that to thermal melting¹⁷. Nonetheless, these studies leave open the question of whether the photoinduced amorphization of Te is nonthermal or thermal.

In this paper, we study the phase transition at low temperatures (down to 80 K) to determine whether tellurium undergoes thermal melting, nonthermal melting, or ultrafast amorphization after high-fluence femtosec-

ond laser excitation. At lower temperatures, higher carrier densities can be optically generated before the lattice temperature reaches its melting point (723 K). The amorphous phase persists for several seconds at room temperature and indefinitely at low temperatures, preventing standard pump-probe measurement methods that involve many laser shots. In our measurements, the time-dependent measurement could be executed in a single shot. Our steady-state and single-shot transient reflectivity studies suggest that the amorphization is the result of thermal melting for all fluences below the ablation threshold.

II. METHOD

The sample was a 250-nm-thick tellurium polycrystalline thin film, sputtered onto a glass slide which was kept in a liquid nitrogen flow cryostat to control its temperature. The details of the single-shot pump-probe setup can be found in the reference¹⁸. The laser source was a Ti:sapphire regenerative amplifier that produced a 2-mJ output pulse energy with 60-fs pulse duration at a repetition rate of 1 kHz. Ninety percent of the pulse energy was sent to a Michelson interferometer to create a pulse pair that was used for double-pumping of the sample. The remaining one-tenth of the energy was used for a probe which was passed through two crossed echelons to form 400 spatially separated beamlets with successive pulses delayed temporally by 23-fs steps. By comparing the probe signal reflected from the sample with and without the pump pulse, a transient reflectivity trace covering 9.2 ps could be acquired with a single pump shot. The change in the steady-state reflectivity long after the sample was pumped was also monitored shot-by-shot by comparing the images without the pump pulse.

III. RESULTS

A. Steady-state reflectivity study

After optical pumping above the amorphization threshold (~ 7 mJ/cm² at 80 K), the irradiated part

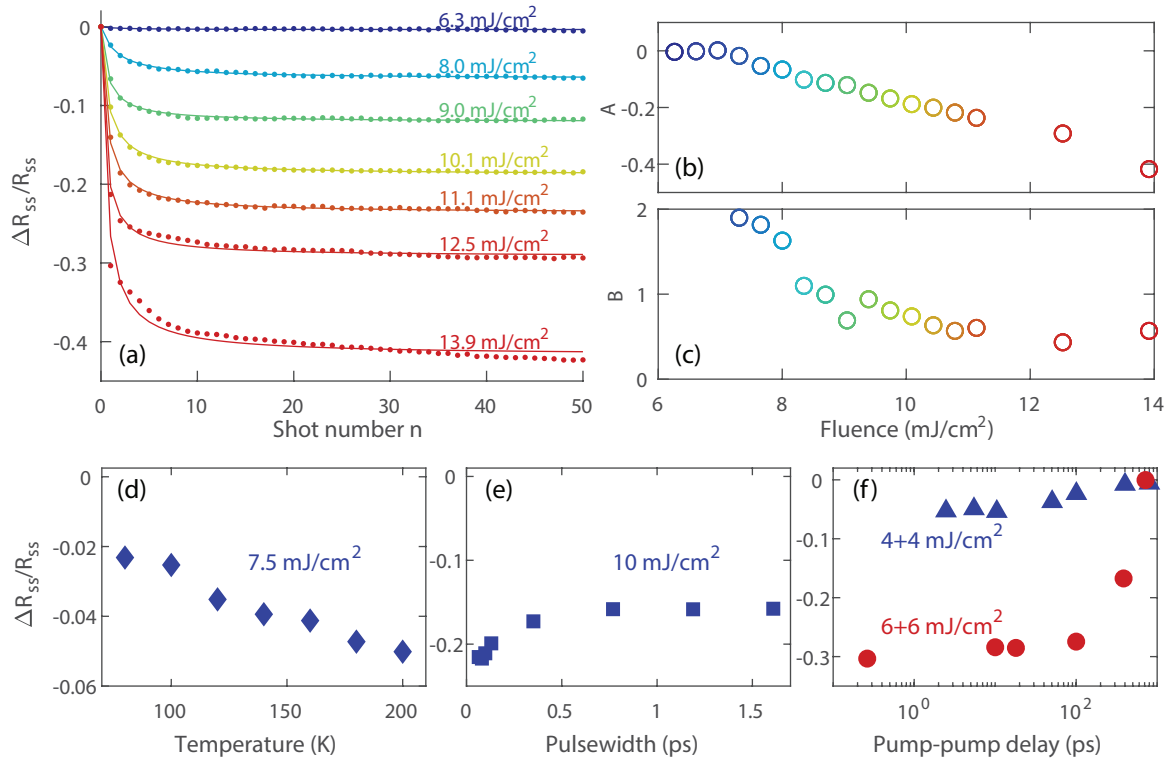


FIG. 1. The change in steady-state reflectivity under single-pump excitation with (a) different pump fluences, (d) different initial temperatures and (e) different pump pulse widths and (f) under double-pump excitation with various pump-pump delays. (a), (e) and (f) were measured at 80 K. (b,c) Parameters used to fit the traces in (a) to $An/(n+B)$. The amorphization threshold is $\sim 7 \text{ mJ}/\text{cm}^2$ and the ablation threshold is $\sim 12 \text{ mJ}/\text{cm}^2$ at 80 K.

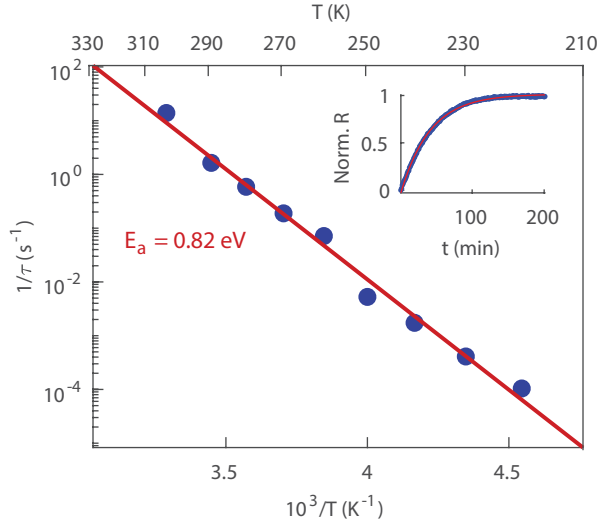


FIG. 2. The estimation of the activation energy from the spontaneous recrystallization rates. (Inset) The recovery dynamics (blue) and the exponential fit (red) at 230 K.

of the film near its surface was turned amorphous and the steady-state reflectivity of the tellurium sample was reduced (photo-darkened). As shown in Fig. 1(a), the amorphization was mostly complete within the first few

pump shots, and the following shots did not change the steady-state reflectivity further, indicating that they did not further significantly increase the volume of the amorphous phase. The threshold and saturation behaviors are common features of photoinduced phase transitions due to the competition of two coexisting phases and the spatial profile of the optical excitation beam¹⁹. For further analysis, we fit the shot-by-shot steady-state reflectivity R_{ss} as a function of the number of shots n to a saturation growth-rate curve,

$$\frac{\Delta R_{ss}}{R_{ss}} = \frac{An}{n+B}, \quad (1)$$

and the fluence-dependent results for the parameters A and B are shown in Fig. 1(b,c). The parameter A represents the saturated change in steady-state reflectivity. Its magnitude increases approximately linearly with pump fluence above the threshold. The parameter B is the number of shots required to reach half the saturation reflectivity change. In GST, atomic force microscopy was used to determine that higher fluences increased both the lateral extent and the depth of amorphous material^{20,21}. For a probe spot size that is smaller than the pump spot size, the fluence-dependent change in reflectivity is influenced by the fraction of amorphous material within the optical penetration depth that contributes to reflection. A linear fluence-dependent growth of the melt depth

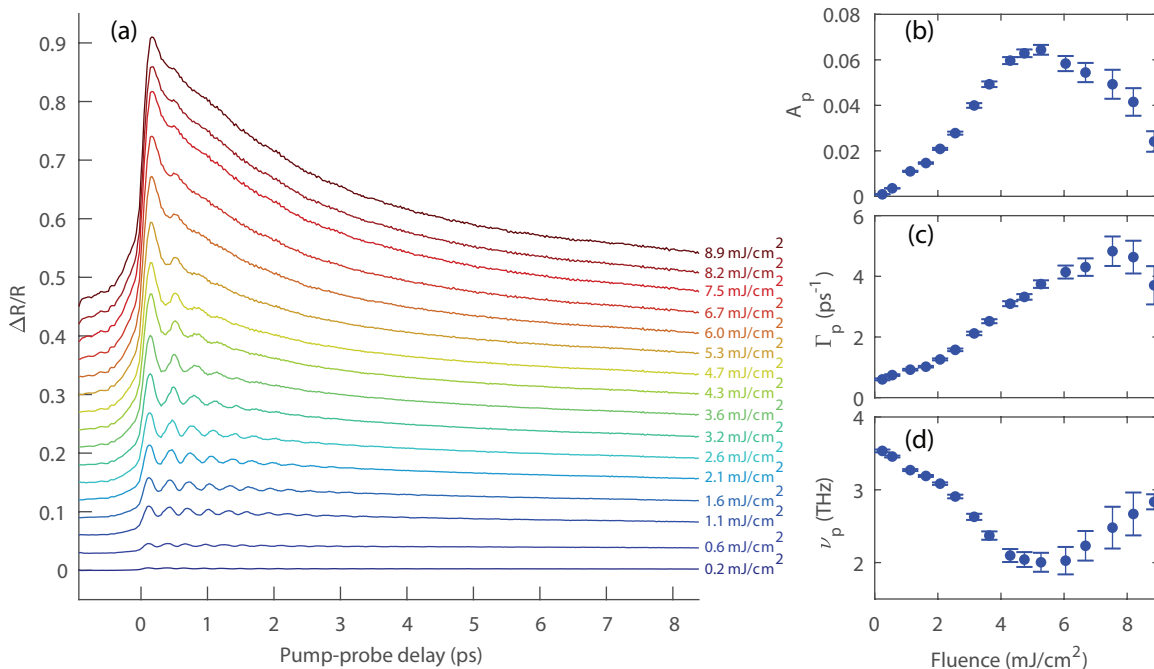


FIG. 3. (a) The transient reflectivity trace under various pump fluences at 300 K. Note the amorphization threshold is ~ 6 mJ/cm^2 at 300 K. (b) The phonon amplitude, (c) damping constant, and (d) phonon frequency obtained by curve fitting.

has been observed in photoexcited tellurium films¹⁴ and might contribute to the linear fluence-dependent change in the steady-state reflectivity observed here.

When exposed with pump fluences above ~ 12 mJ/cm^2 at 80 K, the steady-state reflectivity did not reach a saturation value, but continued to drop (see the deviation from the saturation curve in Fig. 1(a)). We also observed a complete removal of the tellurium film in the illuminated spot after thousands of pump pulses. We attribute this phenomenon to ablation near the surface, which has been previously observed in photoexcited tellurium^{14,17}. The optical pulse did not melt the whole 250-nm film before ablation occurred at the surface¹⁴.

When the sample was kept at low temperatures (< 200 K), the photoinduced amorphous phase was stable and long-lived. At higher temperatures, the amorphous phase relaxed back to the crystalline phase with no visible evidence of change from the initial condition prior to irradiation. We measured the recrystallization dynamics, as indicated by the reflectivity, using a continuous-wave laser and a photodiode. The recovery of the steady-state reflectivity at each temperature is fitted to a single exponential form to determine the recrystallization rate. As shown in Fig. 2, the recrystallization rate at various temperatures fits well to the Arrhenius equation with an activation energy of approximately 0.82 eV.

The recrystallization at low temperatures can be induced by femtosecond pulses with moderate fluences (< 7 mJ/cm^2), demonstrating the feasibility of all-optical switching between the amorphous and crystalline phases using femtosecond pulses. Although one intense pulse

can induce significant amorphization, recrystallization requires multiple weak pulses²². At 80 K, most amorphous regions returned to the crystalline phase after irradiation by 50 pulses with a fluence of 6 mJ/cm^2 ²³, and by more than 4000 shots with 2 mJ/cm^2 fluence. The recrystallization was conducted at a repetition rate of 10 Hz, so accumulated heating was negligible. Therefore, recrystallization is a result of temperature ramping by each pulse.

In order to determine if the amorphization is a result of a thermal process, we varied the initial temperature of the sample and illuminated with the same pump fluence. As shown in Fig. 1(d), the magnitude of the change in steady-state reflectivity increased linearly with the initial temperature. In addition, the amorphization threshold decreased at higher initial temperatures. These behaviors indicate that amorphization is a result of thermal melting, as the heating due to the femtosecond laser pulse adds to the initial sample temperature. A purely non-thermal process would depend only weakly on the initial sample temperature.

To further determine the mechanism of amorphization, we varied the temporal profile of the optical excitation. First, we stretched the pump pulse while fixing the pulse energy. The optical penetration depth δ for 800-nm light is 38 nm¹⁷ and the ambipolar diffusion constant D_e is approximately 40 cm^2/s ²⁶, so the timescale for hot carriers to leave the probed region is $\delta^2/D_e = 0.4$ ps. If the amorphization were induced by a high carrier density, we should see a continuous decrease of the change in steady-state reflectivity as the pulse width becomes much

longer than 1 ps. As shown in Fig. 1(e), the amorphization process is not sensitive to the pulse width except for a slight enhancement at short pulse widths, which can be explained by the local heat dissipation of coherent phonons that are generated before carriers have time to leave the initially excited region, resulting in a larger lattice energy in that region than in the case of longer pulse durations¹⁸. When the pump pulse is shorter than the phonon period, coherent A_1 phonons can be excited and then dissipate the energy into acoustic phonons via anharmonic decay. Without coherent phonon generation, more energy would be transported away from the surface by carrier diffusion, resulting in a lower lattice temperature near the surface.

Second, we excited the sample with two identical but weaker pump pulses, which individually fell below the amorphization threshold but whose sum was sufficient for amorphization. In the high fluence case, the sum of two fluences was near the ablation threshold. As shown in Fig. 1(f), similar degrees of amorphization still occurred when the two pumps were separated by 100 ps, which is sufficient for the majority of excited carriers near the surface to diffuse into the bulk region. Considering the thermal diffusivity $D_l = 3 \times 10^{-6} \text{ m}^2/\text{s}$ ¹⁴, the diffusion time for heat transport out of the initially excited region is approximately $\delta^2/D_l = 500 \text{ ps}$, which is approximately the inter-pulse separation needed to suppress amorphization, and no amorphization was observed when the two pumps were 800 ps apart. Therefore, this phase transition was likely a thermal process rather than nonthermal melting induced by a high density of carriers. In the case of homogeneous melting¹⁷, the lattice temperature was ramped much higher than the melting point in order to overcome the heat of fusion within a few picoseconds, and then the sample entered the solid amorphous phase after fast quenching. It has been shown that there is no significant difference between the optical reflectivity of liquid and amorphous tellurium¹⁴ so we cannot estimate the time of the solidification of the liquid layer with our current data.

B. Transient reflectivity study

In addition to the steady-state reflectivity studies, we can also extract information from transient reflectivity measurements. Fig. 3 shows transient reflectivity traces under different pump fluences, recorded at 300 K. We conducted the experiment at 300 K because the amorphous phase recrystallized completely within a few seconds so that averaging of multiple (~ 100) single-shot sweeps was possible. We observed coherent A_1 phonon oscillations due to displacive excitation by femtosecond pulses^{25,26}. The oscillatory part can be fitted to a chirped damped harmonic oscillation:

$$\frac{\Delta R}{R} = A_p e^{-\Gamma_p t} \cos[2\pi(\nu_0 - \Delta\nu_p e^{-\Gamma t})t + \phi_p]. \quad (2)$$

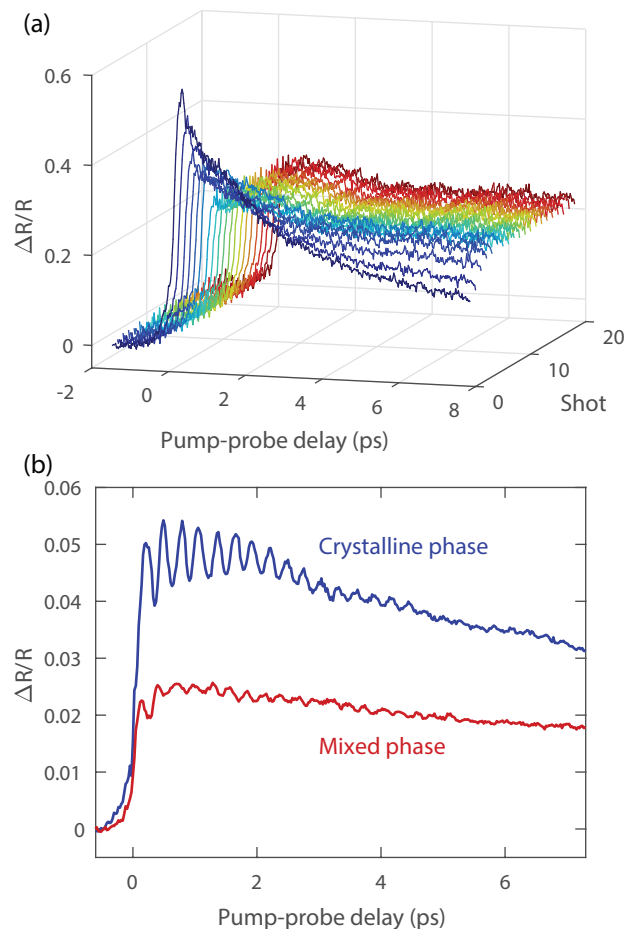


FIG. 4. (a) Shot-by-shot change in transient reflectivity traces with fluence $8.5 \text{ mJ}/\text{cm}^2$ at 80 K. (b) Transient reflectivity with a low pump fluence ($1.3 \text{ mJ}/\text{cm}^2$) before and after amorphization pump pulses ($10 \text{ mJ}/\text{cm}^2$) at 80 K. The oscillation frequency is 3.5 and 3.6 THz respectively.

In the low-fluence regime, as the pump fluence increased, the phonon amplitude A_p increased, the phonon damping rate Γ_p increased, and the phonon frequency $\nu_p = \nu_0 - \Delta\nu_p$ decreased. These effects have been well studied in tellurium below the amorphization threshold using standard pump-probe measurement methods^{24,25,27}. When excited above the amorphization threshold of $\sim 6 \text{ mJ}/\text{cm}^2$, we observed not only the drop of steady-state reflectivity discussed above, but also the strongly damped A_1 mode in the transient reflectivity trace. The existence of coherent phonons suggests that the lattice was not melted within the first picosecond. The drop in the phonon amplitude and the blue shift of the phonon frequency may indicate coherent phonon overshoot of a high-symmetry point²⁸, which could induce amorphization due to disorder in the direction of deviation from the high-symmetry structure. However, since there are few phonon cycles at high fluence, it is difficult to validate such a model based on our present data.

When excited above the amorphization threshold at

low temperatures, the transient reflectivity trace changed shot-by-shot, similar to the steady-state reflectivity. Fig. 4(a) shows the transient reflectivity traces induced by the first 100 shots. Only the first-shot response represented the photoexcited dynamics of the crystalline phase alone. After the first shot, part of the sample near the surface was turned amorphous so the traces excited by later shots represented mixed responses of the photoexcited amorphous phase and the underlying crystalline phase. Since the reflectivity and absorption coefficients near 1.5 eV are both significantly lower in the amorphous state than in the crystalline state^{15,16}, the excitation depth into the sample and the relaxation dynamics of the excited sample depend on the degree of amorphization. Therefore, the transient reflectivity trace induced by the first pump shot when the initial state was entirely crystalline was quite different from those excited by later pump pulses where part of the sample was initially amorphous.

For excitation above the ablation threshold, we observed a single narrow peak along with a decaying background in the transient reflectivity²³. The width of the peak ~ 230 fs is shorter than the A_1 phonon period and a second peak is absent. At this excitation fluence we cannot rule out nonthermal processes contributing to collective structural changes.

Finally, we compared transient reflectivity measurements with low fluences on crystalline and photo-darkened regions at low temperature, as shown in Fig. 4(b). In the crystalline region, the relaxation of $\Delta R/R$ is mainly due to carrier diffusion away from the opti-

cally excited and probed region of the sample. The amorphous phase is expected to have significantly slower carrier diffusion, leading to a far smaller change in $\Delta R/R$ following excitation. The coherent phonon oscillations in the photo-darkened region were suppressed but still could be seen, indicating that we were probing a mixture of crystalline and amorphous states. We note that we did not observe the 150 cm^{-1} oscillation in the amorphous phase as previously seen in the spontaneous Raman spectrum^{10,11}. Such a result might indicate the absence of a chain-like structure in the amorphous phase created by femtosecond pulses²⁹ or a lack of electron-phonon coupling of this Raman mode to electronic excitation.

IV. CONCLUSIONS

In polycrystalline tellurium films, we do not find significant evidence of nonthermal melting or switching behavior with excitation close to twice the amorphization (melting) threshold at low temperature. We believe the photoinduced amorphization is a result of thermal melting followed by rapid quenching of the liquid layer.

ACKNOWLEDGMENTS

This work was supported by National Science Foundation Grants no. 1665383 and by Office of Naval Research Grant no. N00014-12-1-0530.

-
- ¹ S. K. Sundaram and E. Mazur, *Nat. Mater.* **1**, 217 (2002).
² D. von der Linde, K. Sokolowski-Tinten, and J. Bialkowski, *Applied Surface Science* **109-110**, 1 (1997).
³ C. V. Shank, R. Yen, and C. Hirlimann, *Phys. Rev. Lett.* **51**, 900 (1983).
⁴ K. Sokolowski-Tinten, J. Bialkowski, and D. von der Linde, *Phys. Rev. B* **51**, 14186 (1995).
⁵ C. W. Siders, A. Cavalleri, K. Sokolowski-Tinten, C. Tóth, T. Guo, M. Kammler, M. H. v. Hoegen, K. R. Wilson, D. v. d. Linde, and C. P. J. Barty, *Science* **286**, 1340 (1999).
⁶ A. Rousse, C. Rischel, S. Fourmaux, I. Uschmann, S. Sebban, G. Grillon, P. Balcou, E. Förster, J.-P. Geindre, P. Audebert, *et al.*, *Nature* **410**, 65 (2001).
⁷ G. Sciaini, M. Harb, S. G. Kruglik, T. Payer, C. T. Hebeisen, F.-J. M. zu Heringdorf, M. Yamaguchi, M. Horn-von Hoegen, R. Ernstorfer, and R. D. Miller, *Nature* **458**, 56 (2009).
⁸ P. Fons, H. Osawa, A. V. Kolobov, T. Fukaya, M. Suzuki, T. Uruga, N. Kawamura, H. Tanida, and J. Tominaga, *Phys. Rev. B* **82**, 041203 (2010).
⁹ J. Takeda, W. Oba, Y. Minami, T. Saiki, and I. Katayama, *Appl. Phys. Lett.* **104**, 261903 (2014).
¹⁰ M. H. Brodsky, R. J. Gambino, J. E. Smith, and Y. Yacoby, *Phys. Status Solidi (b)* **52**, 609.
¹¹ M. Yashiro and Y. Nishina, in *The Physics of Selenium and Tellurium*, edited by E. Gerlach and P. Grosse (Springer Berlin Heidelberg, Berlin, Heidelberg, 1979) pp. 206–208.
¹² P. C. Clemens, *Appl. Opt.* **22**, 3165 (1983).
¹³ M. Chen, K. A. Rubin, V. Marrello, U. G. Gerber, and V. B. Jipson, *Appl. Phys. Lett.* **46**, 734 (1985).
¹⁴ W. Pamler and E. E. Marinero, *J. Appl. Phys.* **61**, 2294 (1987).
¹⁵ J. Stuke, *J. Non. Cryst. Solids* **4**, 1 (1970).
¹⁶ J. Feinleib and S. Ovshinsky, *J. Non. Cryst. Solids* **4**, 564 (1970).
¹⁷ S. I. Ashitkov, M. B. Agranat, P. S. Kondratenko, S. I. Anisimov, V. E. Fortov, V. V. Temnov, K. Sokolowski-Tinten, B. Rethfeld, P. Zhou, and D. von der Linde, *J. Exp. Theor. Phys. Lett.* **76**, 461 (2002).
¹⁸ Y.-H. Cheng, F. Y. Gao, S. W. Teitelbaum, and K. A. Nelson, *Phys. Rev. B* **96**, 134302 (2017).
¹⁹ J. Zhang, X. Tan, M. Liu, S. W. Teitelbaum, K. W. Post, F. Jin, K. A. Nelson, D. Basov, W. Wu, and R. D. Averitt, *Nat. Mater.* **15**, 956 (2016).
²⁰ V. Weidenhof, I. Friedrich, S. Ziegler, and M. Wuttig, *J. Appl. Phys.* **86**, 5879 (1999).
²¹ V. Weidenhof, N. Pirch, I. Friedrich, S. Ziegler, and M. Wuttig, *J. Appl. Phys.* **88**, 657 (2000).
²² Y. Liu, M. M. Aziz, A. Shalini, C. D. Wright, and R. J. Hicken, *J. Appl. Phys.* **112**, 123526 (2012).

- ²³ See Supplemental Material at [URL will be inserted by publisher] for the shot-by-shot change due to recrystallization and the transient reflectivity traces above the ablation threshold.
- ²⁴ S. Hunsche and H. Kurz, *Appl. Phys. A* **65**, 221 (1997).
- ²⁵ H. J. Zeiger, J. Vidal, T. K. Cheng, E. P. Ippen, G. Dresselhaus, and M. S. Dresselhaus, *Phys. Rev. B* **45**, 768 (1992).
- ²⁶ P. Tangney and S. Fahy, *Phys. Rev. B* **65**, 054302 (2002).
- ²⁷ N. Kamaraju, S. Kumar, M. Anija, and A. K. Sood, *Phys. Rev. B* **82**, 195202 (2010).
- ²⁸ T. Huber, S. O. Mariager, A. Ferrer, H. Schäfer, J. A. Johnson, S. Grübel, A. Lübcke, L. Huber, T. Kubacka, C. Dornes, C. Laulhe, S. Ravy, G. Ingold, P. Beaud, J. Demsar, and S. L. Johnson, *Phys. Rev. Lett.* **113**, 026401 (2014).
- ²⁹ J. Akola and R. O. Jones, *Phys. Rev. B* **85**, 134103 (2012).